Available online at https://link.springer.com/journal/42241
http://www.jhydrodynamics.com
Journal of Hydrodynamics, 2019, 31(1):
https://doi.org/10.1007/s42241-019-0020-6

Development of naoe-FOAM-SJTU solver based on OpenFOAM for marine hydrodynamics *

Jian-hua Wang, Wei-wen Zhao, De-cheng Wan
Collaborative Innovation Center for Advanced Ship and Deep-Sea Exploration, School of Naval Architecture, Ocean and Civil Engineering, State Key Laboratory of Ocean Engineering, Shanghai Jiao Tong University, Shanghai 200240, China

(Received December 23, 2018, Revised January 5, 2019, Accepted January 7, 2019, Published online January 28, 2019)
©China Ship Scientific Research Center 2019

Abstract: A CFD solver naoe-FOAM-SJTU (The abbreviation naoe stands for naval architecture and ocean engineering) is developed based on the open source platform OpenFOAM with the purpose of simulating various marine hydrodynamic problems. In the present paper, self-developed modules, i.e., wave generation and absorption, 6 degrees of freedom motion, mooring system, dynamic overset grid, fluid-structure interaction, unsteady actuator line model, implemented on the open source platform OpenFOAM are introduced to illustrate the development of the marine hydrodynamics CFD solver. Furthermore, extensive simulations of marine hydrodynamic problems using the developed modules are conducted and validated by available experimental data. It has been proved that the CFD solver naoe-FOAM-SJTU is suitable and reliable in predicting the complex viscous flow around ship and offshore structures. Efficiency and accuracy need to be focused in the future development of the present CFD solver.

Key words: Marine hydrodynamics, fluid-structure interaction, overset grid, naoe-FOAM-SJTU solver, OpenFOAM

Introduction

OpenFOAM[1] is the leading free, open source software for computational fluid dynamics and other computational science and engineering. Jasak[2] demonstrates the main features of the open source library with a very deep insight into the design of the code structure, where the object orientation and basic classes in OpenFOAM are introduced. OpenFOAM has implemented the basic modules, such as mesh motion handling, linear system and solver support, discretization schemes and physical models in library form. Based on the above modules, many top-level solvers are utilized to deal with fluid dynamic problems in many research fields. So far, OpenFOAM has been successfully applied to the numerical studies of heat transfer[3-4], coastal engineering[5], porous media[6], turbulence modelling[7], compressible flows[8], free surface flows[9], ocean engineering[10], etc.. With the advantage of the flexibility of solver customization, OpenFOAM has been chosen as the priority toolbox by the researchers in the field of computational fluid dynamics (CFD).

Over the past two decades, OpenFOAM has been extended to a large number of functional modules, such as dynamic mesh handling[11], pre and post processing utilities, etc.. Despite the abundant libraries of OpenFOAM, there are still a lot of work need to be done in order to meet the requirement of specific engineering problems. For the marine engineering, such as violent free surface waves, complex motions with ship hull-propeller-rudder interaction, large amplitude platform motions with mooring lines, vortex-induced vibration (VIV) of marine risers, floating offshore wind turbine in ocean waves and so on, there is a lack of available solvers to handle such complex situations in the OpenFOAM released versions. Therefore, it is very essential to develop specialized modules in OpenFOAM to investigate the hydrodynamic performance of marine engineering problems. In the present paper, emphasis is put on the development of the naoe-FOAM-SJTU solver for complex flows in marine hydrodynamics. The recent progress of naoe-FOAM-SJTU solver is overviewed

* Project supported National Natural Science Foundation of China (Grnt Nos. 51809169, 51879159, 51490675, 11432009 and 51579145).
Biography: Jian-hua Wang (1988-), Male, Ph. D., Assistant Professor, E-mail: jianhuawang@sjtu.edu.cn
Corresponding author: De-cheng Wan, E-mail: dcwan@sjtu.edu.cn

based specifically on the developed hydrodynamic CFD modules with various marine engineering applications. The naoe-FOAM-SJTU solver, which is developed by the Computational Marine Hydrodynamics Lab (CMHL) in Shanghai Jiao Tong University (SJTU), can be used as an alternative tool to estimate the hydrodynamic performance of ship and offshore structures. It can also be utilized to obtain a better understanding of the complex physics in marine engineering.

The main content of this paper comes from the keynote lecture "Progress of naoe-FOAM-SJTU solver for marine hydrodynamics" presented at the 13th OpenFOAM Workshop (OFW13, the workshop website can be found in the last page). The annual Open- FOAM Workshop is the most important and influential forum for researchers and users from universities, institutes as well as industries to promote collaborative activities and share latest progresses on OpenFOAM in many areas. It is an attractive community event opening to scientists, scholars, engineers, students, users and contributors, regardless of their background and avocations. In 2006, the 1st OpenFOAM Workshop (OFW1) was held in Zagreb, Croatia. Since then it was held every year successively in Zagreb, Milan, Montréal, Gothenburg, Pennsylvania, Darmstadt, Jeju, Zagreb, Ann Arbor, Guimarães and Exeter, respectively. The 13th OpenFOAM Workshop was held in Shanghai, China, on June 24-29, 2018, and hosted and organized by Shanghai Jiao Tong University, and co-organized by Journal of Hydrodynamics, Shanghai Key Laboratory of Ship Engineering, and State Key Laboratory of Navigation and Safety Technology. Prof. Decheng Wan was conference chair of the 13th OpenFOAM Workshop.

It is the first time that the OpenFOAM Workshop is held in China. There are more than 300 participants from over 25 countries to attend the OFW13 and making it the largest number of attendees in its history. Over 260 papers were received in OFW13 and 133 papers were accepted after the peer-review, in which 106 papers were chosen for presentations in parallel sessions during the 4 days' workshop. Five keynote lectures were given by Prof. Hrvoje Jasak (the original Co-Author of OpenFOAM) from the university of Zagreb, Prof. Gavin Tabor from the university of Exeter, Prof. Francois Guibault from Ecole Polytechnique de Montreal, Prof. Xinhai Xu from National Innovation Institute of Defense Technology and Dr. Jian-hua Wang from SJTU, respectively. 15 training sessions led by experienced code developers were held for all the attendees. Poster presentations contributed by the participants were exhibited in the venue during the workshop. 44 parallel sessions were organised and the presentations were classified into different research fields related to OpenFOAM, namely, naval hydrodynamics, coastal/offshore engineering, aerodynamics, civil engineering, fluid-structure interaction, general CFD, phase change, multiphase flows, heat transfer, reacting flows, turbulence modelling, sprays and injection, porous media, optimization and control, turbomachinery, complex materials. A session of pre/post-processing, meshing and user environments was also arranged during the workshop. Mini-symposiums on specified themes were held at the last day of OFW13 and topics on numerical tank for ship and offshore structures, Paraview features, floating offshore wind turbines were discussed in-depth by participants related to the corresponding research areas. The 13th OpenFOAM Workshop held in Shanghai, China is very successful and it gives an opportunity for researchers in the field of computational fluid dynamics from all over the world to exchange ideas and follow-up the recent progresses related to OpenFOAM.

1. OpenFOAM features for marine hydrodynamics

OpenFOAM is more likely a framework than a CFD package. It provides quantities of features which can be used to construct solvers for specific industrial problems. This section introduces several existing features in OpenFOAM that are incorporated into the naoe-FOAM-SJTU solver.

1.1 *Flow modelling*

In the field of naval architecture and marine engineering, fluid is treated as incompressible flow. If the free surface effect is insignificant, such as propeller open water test and performance of marine risers, the flow can be modelled as single-phase flow. However, if the free surface effect is not neglectable, such as the prediction for strong wave-structure interaction, ship wave-making resistance, then the interface must be considered in the simulation. OpenFOAM has already provided physical models for these two types of fluid flow.

For single-phase flow, the governing equations are the continuity and unsteady Reynolds-averaged Navier-Stokes (URANS)/detached-eddy simulation (DES) equations. These equations in an arbitrary Lagrangian-Eulerian (ALE) form can be written as:

$$\nabla \cdot \boldsymbol{U} = 0 \tag{1}$$

$$\frac{\partial \boldsymbol{U}}{\partial t} + \nabla \cdot [(\boldsymbol{U} - \boldsymbol{U}_g)\boldsymbol{U}] = -\frac{1}{\rho}\nabla p + \nabla \cdot \boldsymbol{R}_{\text{eff}} \tag{2}$$

where $\boldsymbol{U}$, $\boldsymbol{U}_g$ are the velocity of flow field and mesh cells, respectively, p is the pressure and ρ is the fluid density, $\boldsymbol{R}_{\text{eff}} = \nu_{\text{eff}}[\nabla \boldsymbol{U} + (\nabla \boldsymbol{U})^{\text{T}}]$ is the

effective Reynolds stress tensor with $\nu_{\text{eff}} = \nu + \nu_t$ the effective kinematic viscosity of fluid, in which ν, ν_t are kinematic and eddy viscosity, respectively.

While for flow that involves free surface, OpenFOAM utilizes an algebraic volume of fluid (VOF) method to capture the interface. The governing equations for incompressible, immiscible two-phase flow hence becomes:

$$\nabla \cdot \boldsymbol{U} = 0 \tag{3}$$

$$\frac{\partial \rho \boldsymbol{U}}{\partial t} + \nabla \cdot [\rho(\boldsymbol{U} - \boldsymbol{U}_g)\boldsymbol{U}] = -\nabla p_d - \boldsymbol{g} \cdot \boldsymbol{x} \nabla \rho + \nabla \cdot (\mu_{\text{eff}} \nabla \boldsymbol{U}) + \nabla \mathbf{U} \cdot \nabla \mu_{\text{eff}} + \boldsymbol{f}_\sigma \tag{4}$$

where p_d is the dynamic pressure of flow field obtained by subtracting the hydrostatic part $\rho \boldsymbol{g} \cdot \boldsymbol{x}$ from total pressure, $\boldsymbol{g}$ is gravitational acceleration vector, $\mu_{\text{eff}} = \rho \nu_{\text{eff}}$ denotes the effective dynamic viscosity of fluid, $\boldsymbol{f}_\sigma = \sigma \kappa \nabla \alpha$ is the source term for surface tension, with σ the surface tension coefficient, κ the mean curvature of the interface and α the volume fraction. In OpenFOAM, VOF method with bounded compression technique[12] is applied to capture free surface and the transport equation is expressed as

$$\frac{\partial \alpha}{\partial t} + \nabla \cdot [(\boldsymbol{U} - \boldsymbol{U}_g)\alpha] + \nabla \cdot [\boldsymbol{U}_r (1-\alpha)\alpha] = 0 \tag{5}$$

where α is volume of fraction, 0 and 1 represent that the cell is filled with air and water respectively and $0 < \alpha < 1$ stands for the interface between two-phase fluid. $\boldsymbol{U}_r$ is the velocity field used to compress the interface and it only takes effect on the free surface due to the term $(1-\alpha)\alpha$.

Currently, the naoe-FOAM-SJTU solver supports k-ω SST and k-ω SST DES/DDES model. The eddy viscosity in these models are calculated by

$$\nu_t = \frac{a_1 k}{\max(a_1 \omega, F_2 \Omega)} \tag{6}$$

in which k, ω are turbulence kinetic energy (TKE) and specific turbulence dissipation rate, respectively, a_1 is model coefficient, F_2 is the blending function, Ω is the vorticity.

For URANS, the k and ω are solved by the following transport equations[13]:

$$\frac{\partial (\rho k)}{\partial t} + \nabla \cdot (\rho k \boldsymbol{U}) = \rho \tilde{G} - \rho \frac{k^{3/2}}{l_{\text{RANS}}} + \nabla \cdot [\rho(\nu + \alpha_k \nu_t) \nabla k] \tag{7}$$

$$\frac{\partial (\rho \omega)}{\partial t} + \nabla \cdot (\rho \omega \boldsymbol{U}) = \rho \gamma S^2 - \rho \beta \omega^2 + \nabla \cdot [\rho(\nu + \alpha_\omega \nu_t) \nabla \omega] + \rho(1 - F_1) C D_{k\omega} \tag{8}$$

where $l_{\text{RANS}} = \sqrt{k} / (\beta^* \omega)$ is the RANS turbulent length scale.

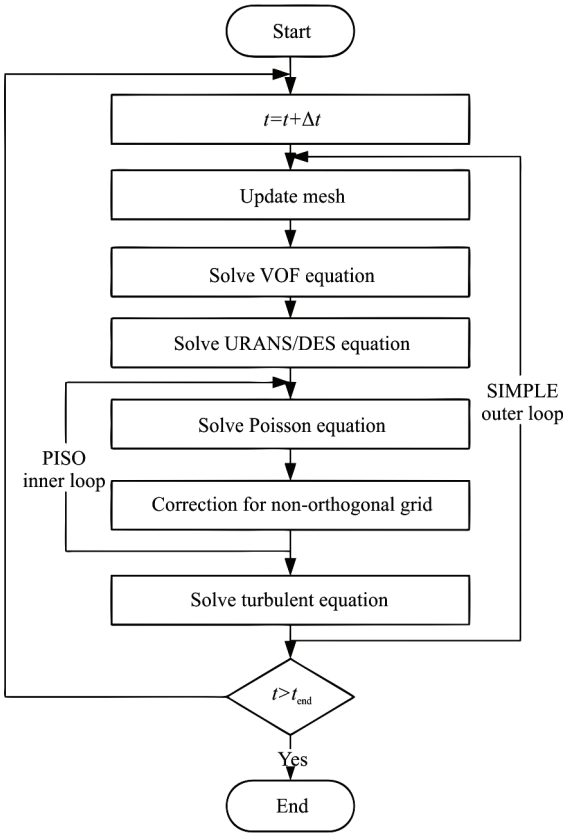

Fig. 1 Flowchart of the PIMPLE algorithm

The k-ω SST DES/DDES modifies the length scale to become l_{DES} and l_{DDES}, respectively, defined as:

$$l_{\text{DES}} = \min(C_{\text{DES}} \Delta, l_{\text{RANS}}) \tag{9}$$

$$l_{\text{DDES}} = l_{\text{RANS}} - f_d \max(0, l_{\text{RANS}} - C_{\text{DES}} \Delta) \tag{10}$$

in which C_{DES} is the calibrated DES constant, Δ is the grid scale, f_d is a delayed function which

ensures that DES works in RANS manner inside boundary layer to avoid grid-induced separation (GIS).

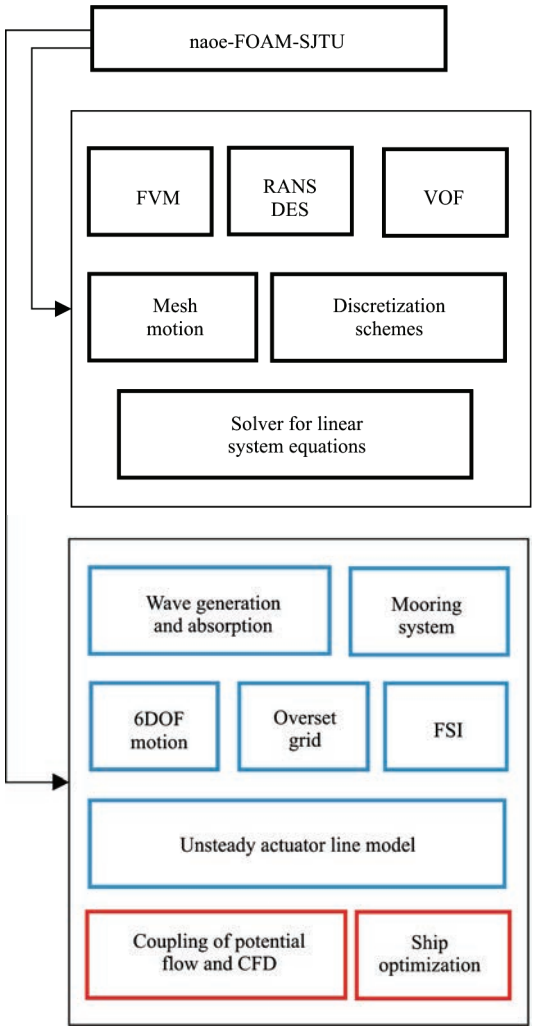

Fig. 2 (Color online) Main framework of naoe-FOAM-SJTU solver

1.2 *Numerical schemes*

For incompressible flow, there is no explicit coupling between velocity and pressure. The naoe-FOAM-SJTU solver employs a segregated method named PIMPLE to decouple velocity and pressure. PIMPLE is a combination of the SIMPLE and PISO[14] algorithm which provided by OpenFOAM. Figure 1 depicts the flowchart of the PIMPLE algorithm. When advancing to a new time step, the solver first update mesh, then solve momentum equations to get an intermediate velocity which is used to construct the pressure Poisson equation later. After that, the solver enters PISO loop, solves for pressure and performs non-orthogonal correction several times. Then the velocity and flux are corrected and the solver enters the next SIMPLE iteration. For flow with free surface, an extra VOF transport equation should be solved before URANS/DES equations. The procedure is also depicted in the flowchart.

The naoe-FOAM-SJTU solver also utilizes discretization schemes from OpenFOAM. The most commonly used schemes are introduced below. For temporal terms, a second order backward scheme is used. This scheme uses the values of previous two time steps for discretization. As for convection terms, care should be taken for URANS and DES. URANS can use *limitedLinear* for both momentum equations and turbulence transport equations. While DES can use *LUST* for momentum equations and *limitedLinear* for turbulence transport equations. In addition to the built-in discretization schemes, OpenFOAM also provide a large number of solvers for the linear system of equations.

2. Main modules of naoe-FOAM-SJTU

Based on the supported features in OpenFOAM mentioned above, the development for marine hydrodynamics CFD solver is mainly through the implementation of specific modules. Figure 2 demonstrates the main framework of the present CFD solver naoe-FOAM-SJTU. As mentioned in introduction part, the CFD solver is developed based on open source platform OpenFOAM and the built-in modules, such as finite volume method (FVM), discretization schemes, solver for linear system equations. Further implementation of marine hydrodynamic modules in the solver is shown in the right column of Fig. 2, where the blue marked modules are already developed and modules in red are the ongoing work at present.

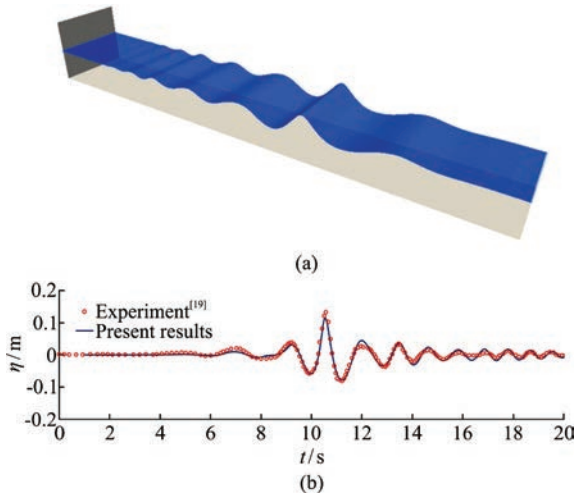

Fig. 3 (Color online) Freak wave generation using flap type wavemaker and comparison with experimental measurement[19]

2.1 *Wave generation and absorption*

For a marine hydrodynamic problem, wave envi-

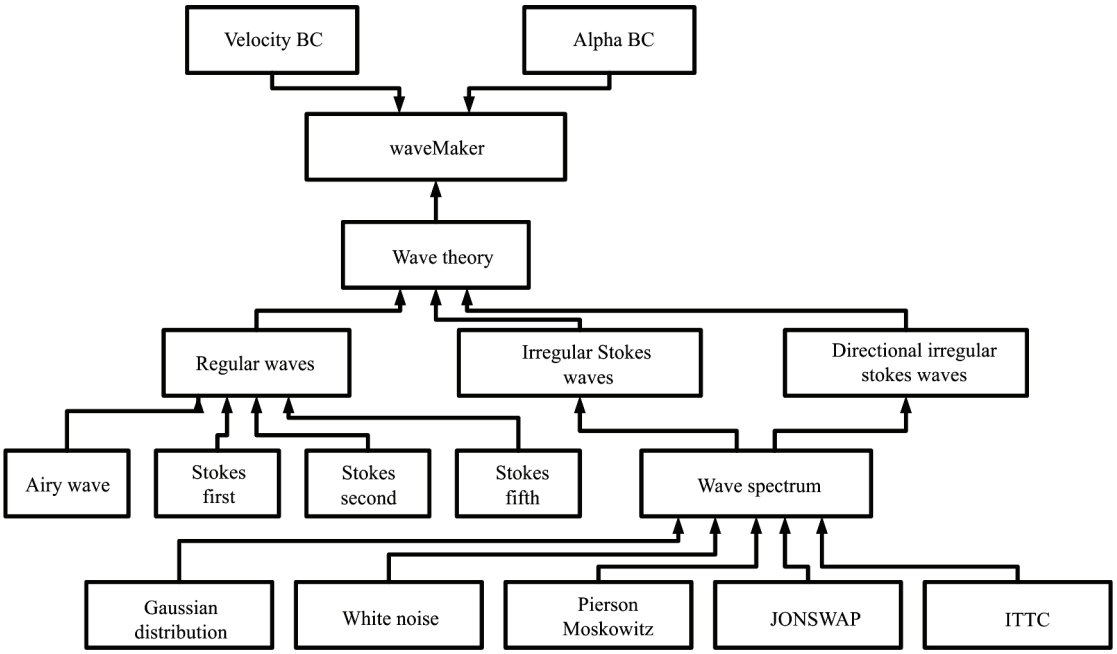

Fig. 4 Code structure of wave generation module based on boundary conditions

ronment is the most typical situation for offshore floating structures. Therefore, ocean wave generation is the first job to be done for the development of a marine hydrodynamic CFD solver. So far, there have already been several modules developed based on OpenFOAM, such as waves2foam[9], olaFlow[5, 15]. Two wave generation approaches[16-18] are implemented in naoe-FOAM-SJTU, one is the modelling of a piston or flap type wavemaker, another one is the velocity-inlet boundary conditions. For a piston or flap type wavemaker, the main implementation is to give the prescribed wave profile to the movement of the wave boundary incorporated with the moving mesh technique[11] in OpenFOAM. This procedure is usually used to generate regular waves, solitary waves, freak waves just like a the wavemaker in an actual wave basin. Figure 3 presents the numerical prediction of a freak wave generated by the flap type wave maker using naoe-FOAM-SJTU and the simulated results are validated by the available experiments[19].

The inlet boundary condition type wavemaker imposes both the velocity of water particles and the position of free surface at the incident wave boundary. Figure 4 illustrates the code structure of wave generation module in naoe-FOAM-SJTU solver.

It can be seen from Fig. 5 that the present inlet BC type wave maker can generate both regular and irregular waves according to corresponding wave theories. Regular waves varying from the airy wave to the fifth-order Stokes waves as well as shallow water waves can be generated. For irregular waves, a wave spectrum based correction approach[20] is implemented in the present wave generation module. The most frequently used spectrum, such as PM, JONSWAP, one/two parameter ITTC, are implemented to the present solver to extend the ability of generating ocean waves. In addition, the directional irregular waves are also implemented by multiplying the directional spreading function with wave spectrum. The detailed implementation is shown in the Ref. [17] and 3-D focusing wave and multidirectional nonlinear waves are validated by comparing present predictions with available experimental results.

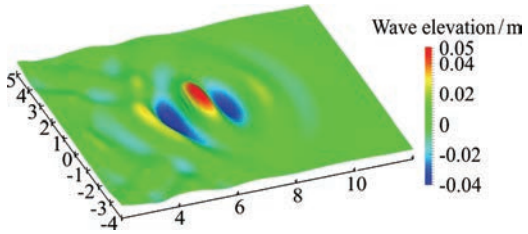

Fig. 5 (Color online) Instantaneous free surface of multidirectional focusing wave[17]

Apart from the wave generation module, a wave absorption module based on sponge layer is implemented in the present CFD solver. The sponge layer is developed by Cao et al.[21] and worked effectively in previous studies. The methodology adopts a source term $f_s(x)$ and is added in the momentum equation. The term is denoted as:

$$f_s(x) = -\rho\alpha_s\left(\frac{x - x_s}{L_s}\right)^2 (\boldsymbol{U} - \boldsymbol{U}_{\text{ref}}) \tag{11a}$$

$$f_s(x) = 0 \tag{11b}$$

where α_s denotes the damping coefficient and x_s represents the start position of wave damping zone and L_s stands for the length of the damping zone.

2.2 *6DOF motion*

After implementing the wave generation and absorption module, a six-degrees-of-freedom (6DOF) motion module is required in order to estimate the motion response for ship and offshore structures in sea environment. Basically, there are two approaches to describe the motion of a rigid floating body, i.e., quaternion and Euler angle. In our present solver, the 6DOF motion module is developed based on the Euler angle description, where two coordinate systems, i.e., earth-fixed coordinate system and ship-fixed coordinate system, are employed to calculate the rigid body motions. The 6DOF motion equations are presented as:

$$\dot{u} = \frac{X_s}{m} + vr - wq + x_g(q^2 + r^2) - y_g(pq - \dot{r}) - z_g(pr + \dot{q}) \tag{12a}$$

$$\dot{v} = \frac{Y_s}{m} + wp - ur + y_g(r^2 + p^2) - z_g(qr - \dot{p}) - x_g(qp + \dot{r}) \tag{12b}$$

$$\dot{w} = \frac{Z_s}{m} + uq - vp + z_g(p^2 + q^2) - x_g(rp - \dot{q}) - y_g(rp + \dot{p}) \tag{12c}$$

$$\dot{p} = \frac{1}{I_x}\{K_s - (I_z - I_y)qr - m[y_g(\dot{w} - uq + vp) - z_g(\dot{v} - wp + ur)] \tag{12d}$$

$$\dot{q} = \frac{1}{I_y}\{M_s - (I_x - I_z)rp - m[z_g(\dot{u} - vr + wq) - x_g(\dot{w} - uq + vp)]\} \tag{12e}$$

$$\dot{r} = \frac{1}{I_z}\{N_s - (I_y - I_x)pq - m[x_g(\dot{v} - wp + ur) - y_g(\dot{u} - vr + wq)]\} \tag{12f}$$

where the left side terms are the accelerations of body motions. The calculation procedure for a rigid floating body is shown in Fig. 6. During the 6DOF computation, the forces and moments are first computed in the earth-fixed coordinate system. Then the predicted values are transformed into ship-fixed coordinate system for the calculation of accelerations. After that, the accelerations are integrated to obtain the ship velocities, which are then transformed back to earth-fixed coordinate system to get the ship displacement by integrating the velocities.

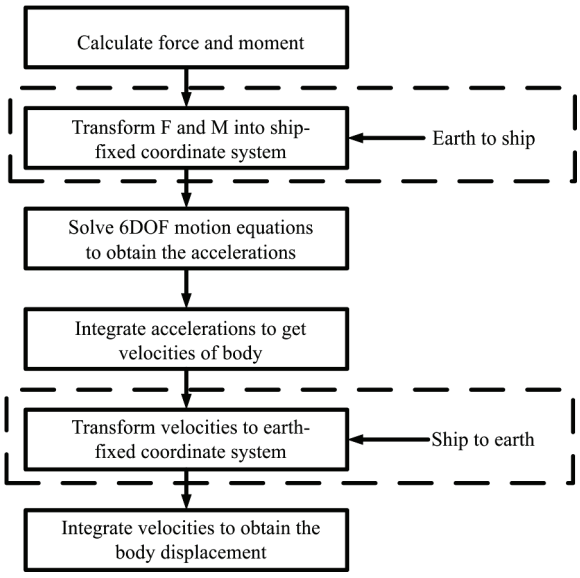

Fig. 6 Procedure of 6DOF motion module in naoe-FOAM-SJTU

The 6DOF motion module discussed above is developed to compute the motion response of ship and offshore platforms[22-23]. When considering the complex motions of free running ship or floating offshore wind turbines, where the ship hull-propeller-rudder interaction and turbine-platform interaction should be taken into account, the motion module then needs to be updated to meet the requirement of multi-level motions.

In our present solver, full 6DOF motion module with a hierarchy of bodies is implemented[24]. For a free running ship, the rotating propeller or turning rudder are the children level motion based on the ship hull motion. Similarly, the rotating turbine is the sub-level of the platform motion. Figure 7 illustrates the motion level of ship and offshore platforms. The strategies to compute the movements of propeller, rudder, turbine and other appendages depend on the problem to solve. For example, for a self-propulsion simulation, the rotation of propeller is updated by a PI

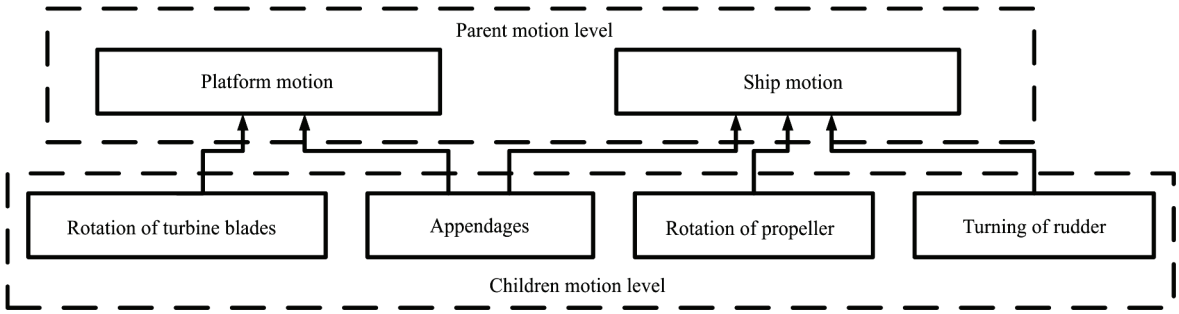

Fig. 7 Full 6DOF motion with a hierarchy of bodies

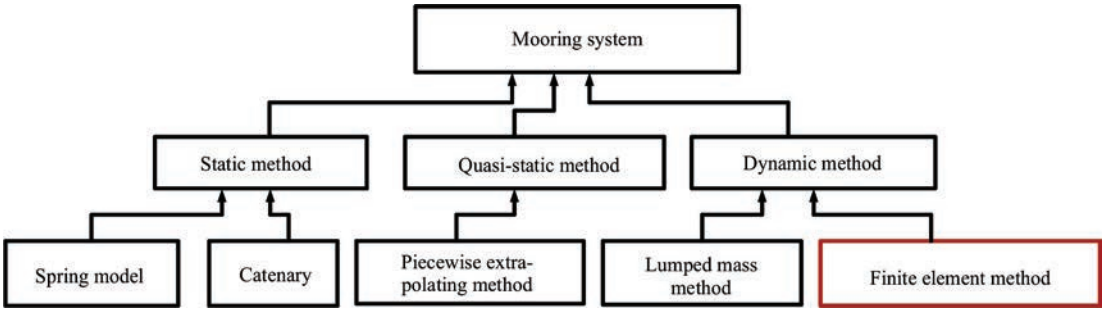

Fig. 8 (Color online) Framework of mooring system module

controller. While for a turning circle maneuver, the movement of rudder is executed by the turning controller. The full 6DOF motion module with a hierarchy of bodies can be used to simulate various complex conditions in marine engineering incorporating with the dynamic overset grid method (see in Section 2.4).

2.3 *Mooring system*

Mooring systems are widely used in marine engineering to keep the stability of floating bodies in ocean waves. In the present solver, a mooring system module is developed based on OpenFOAM and several types of mooring lines are implemented. The framework of the mooring system module in the naoe-FOAM-SJTU solver is shown in Fig. 8. The spring model in the present implementation involves three types, i.e., a linear spring with constant factor k following Hooke's law, a discontinuous spring with different k in several segments and a compressible spring, which can provide restoring force when the length is smaller than the initial. As for the quasi-static approach, a pricewise extrapolating method (PEM)[25] is adopted to discretize the mooring line into a number of segments, where the equations of static equilibrium for each segment is solved. In addition, the PEM approach can consider the different structural properties for mooring lines consist of different components. Both the static and quasi-static method ignore the effect of mooring line movement. Thus, a dynamic module including 3-D lumped mass method (LMM) and finite element method (FEM) is also implemented, in which the development of finite element method is ongoing. The restoring force of mooring lines computed by LMM and FEM approach is obtained by solving the dynamic equations of motion, where the inertial force related with mooring line motion can be considered. The present mooring system module has been applied to predict mooring forces of various floating structures in wave environments[23, 26-28].

2.4 *Overset grid*

As mentioned in Section 2.2, complex motions of multi-systems are the main features of marine structures. Large amplitude body motions are occurred when the floating body encounters violent sea states. Traditional mesh motion handling strategy, such as deforming mesh, cannot maintain the grid quality and even diverged when conducting such large or complex motion simulations. Thus, it is very essential to develop the overset grid module to extend the ability of present CFD solver for directly simulating the complex motions in marine engineering.

A typical demonstration of overset grids used in ship hull-propeller-rudder system is depicted in Fig. 9. Generally, overset grids include multi-blocks of overlapping structured or unstructured grids, and each block can move independently without any constraints. The connectivity of overlapping cells is obtained by

interpolation of neighbour cell. As shown in Fig. 10, fringe cells will get the fluid data through interpolation of donor cells. Detailed information of the overset grid method can be found in pervious publications using naoe-FOAM-SJTU[24, 29-31].

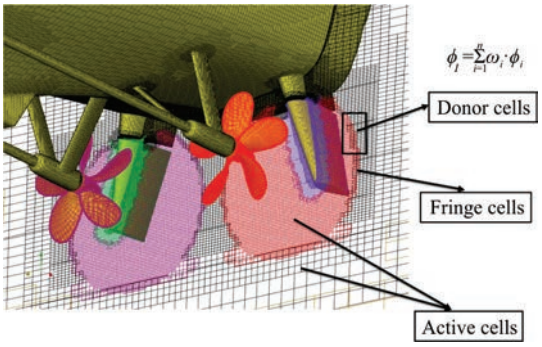

Fig. 9 (Color online) Overset grid demonstration for ship hull-propeller-rudder system

The implementation of the overset grid module in the naoe-FOAM-SJTU solver is accomplished by Shen et al.[24]. Suggar++[32] program is utilized to calculate the overset grid connectivity information (DCI) at run time. DCI manipulation in OpenFOAM is achieved by encapsulating the functions to an overset library liboverset.so. Two public member functions, i.e. updateFvMatrix and updateFvField, are used to modify the sparse matrix solvers and MULES solver by excluding the non-active cells. The parallel coupling strategy between flow and DCI calculations is using the lagged mode[24, 33]. Another feature of the present overset grid module is the association with 6DOF motion with a hierarchy of moving components (see in Section 2.2).

2.5 *Fluid-structure interaction*

With the depth of oil and gas exploitation increases, the aspect ratio of marine riser increases apparently and the flexibility of the marine riser becomes non-negligible. VIV of the flexible riser is one of the main sources of failure damage that has been investigated extensively during the past decades in marine engineering. For a long flexible riser, the three-dimensional simulations will cost a mass of computational resources. In order to predict the VIV response of the flexible riser more effective, the strip theory method proposed by Willden and Graham[34-35] is adopted in our present CFD solver. The methodology has been validated by Yamamoto et al.[36], Meneghini et al.[37] .

A fluid-structure interaction (FSI) module based on the strip method and OpenFOAM are implemented in the present CFD solver naoe-FOAM-SJTU. The FSI module is design for predicting VIV response of the flexible riser in marine engineering. Figures 10, 11 show the layout of the strip theory and the framework of the FSI module respectively. In the fluid field module, the three-dimensional flow field is simplified into several two-dimensional strips distributed equidistantly along the span of the riser. The hydrodynamic forces in both crossflow and inline directions are computed from each fluid strip using the built-in RANS approach in OpenFOAM. Then, the hydrodynamic forces will be transformed into uniformly distributed load acting on the riser. The structural vibration of the riser is calculated through the finite element method (FEM) with the Euler-Bernoulli bending beam model in both directions. After that, the nodal displacements will be transferred to the dynamic mesh and update it for computation in the next time step.

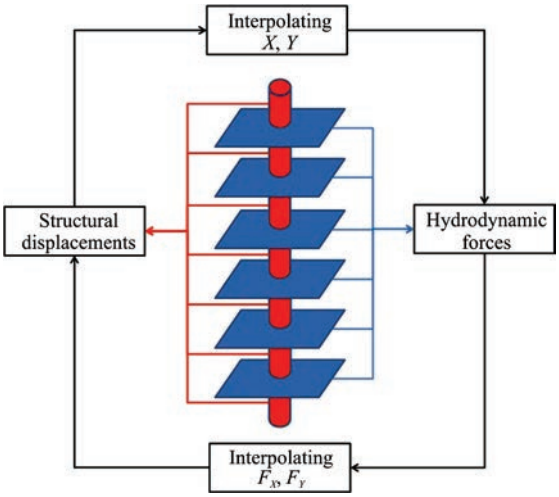

Fig. 10 (Color online) Schematic diagram of the strip method

The present strip method is very appropriate for solving FSI problems with supramaximal computational domain. It owns high computational efficiency and the accuracy is reliable compared with the semi-empirical formula method. The reliability of the module has been verified by Duanmu et al.[38], in which the benchmark case has been analysed detailly compared with experimental results. Furthermore, extensive simulations[10, 38-40] on VIV are conducted for a flexible riser experiencing uniform, shear and stepped respectively.

2.6 *Unsteady actuator line model*

The actuator line model (ALM) is a simplified way to implement the aerodynamic prediction of wind turbine, which is developed by Sørensen and Shen[41]. In the ALM, the real blades surfaces are replaced with virtual actuator lines (shown in Fig. 12), thus the blade geometry layer can be neglected. The wind turbine blades are simplified into actuator lines withstanding body forces, which are divided into a series of discrete

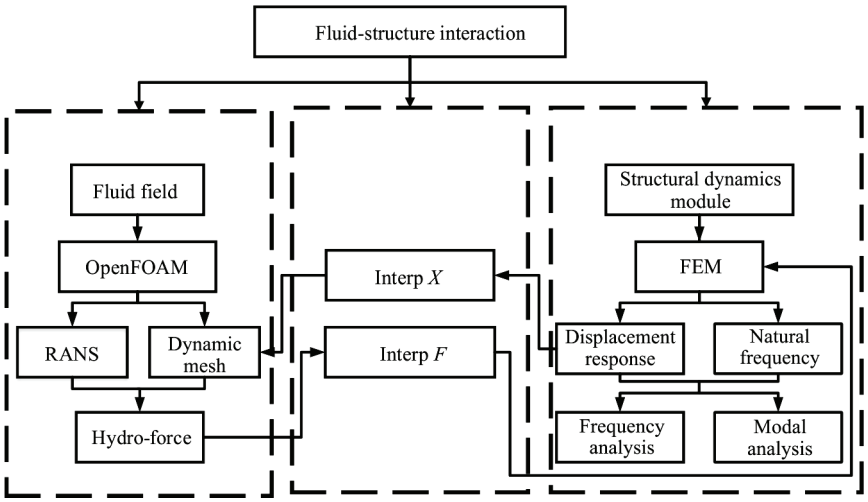

Fig. 11 Framework of fluid-structure interaction module

actuator points. The body forces acting on these actuator points can be calculated using a local velocity and two-dimensional airfoil data. The calculated body force is smeared by using a Gaussian function to avoid singular behavior in numerical calculations. Then the smeared body forces are introduced into the moment equations as a source term to reproduce the turbulent wake flow of wind turbine.

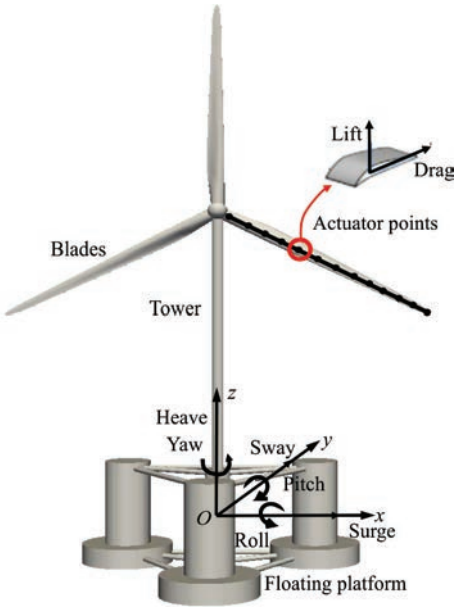

Fig. 12 Demonstration of unsteady actuator line model for floating offshore wind turbines

When the ALM is applied to model the unsteady aerodynamics of floating offshore wind turbines (FOWTs), some modifications should be made to consider the influence of floating platform motions. This is accomplished by introducing an additional velocity vector induced by the platform motion into the calculation of local velocity at blade section. Figure 12 illustrates the actuator line model applied in the floating offshore wind turbine. The unsteady actuator line model[42] (UALM) are developed for the aerodynamic predictions of the FOWT. By combining the UALM and naoe-FOAM-SJTU solver, a coupled CFD analysis tool is established for aero-hydrodynamic simulation of the FOWTs under wind-wave conditions (shown in Fig. 13). The unsteady aerodynamics are predicted by the UALM, and the naoe-FOAM-SJTU solver is employed to obtain the hydrodynamic loads, mooring forces and the platform motions.

To achieve the coupling between the wind turbine aerodynamics and floating platform hydrodynamics, there are data exchange between the UALM module and naoe-FOAM-SJTU solver. To reflect the influence of wind turbine on the hydrodynamics of floating platform, body forces calculated from the UALM module are introduced into the 6DOF motion equations. And the platform position and velocities at each time step obtained from naoe-FOAM-SJTU solver are delivered to the calculation of wind turbine body force.

3. Applications

Main modules in naoe-FOAM-SJTU solver for marine hydrodynamics have been introduced in the previous section. Based on the CFD solver associated with featured modules, extensive applications have been carried out in marine hydrodynamic problems including ship hydrodynamics, offshore platform in ocean engineering, marine risers, floating offshore wind turbines, and so on. This section mainly focuses on the engineering applications using the present CFD solver. Discussions and analysis for the flow field regarding to typical cases are involved in each part.

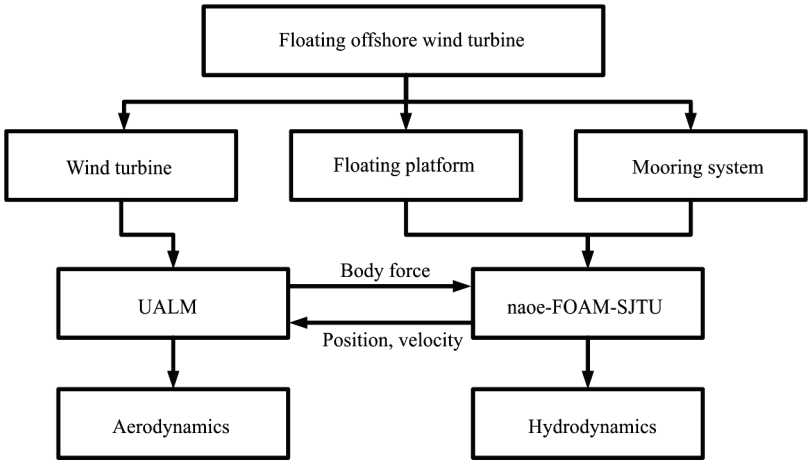

Fig. 13 Coupling between unsteady actuator line model and naoe-FOAM-SJTU

3.1 *Ship hydrodynamics*

So far, various applications to ship hydrodynamics have been done using the self-developed CFD solver naoe-FOAM-SJTU. Ship resistance in calm water is the most fundamental study in ship hydrodynamics and several benchmark computations have been carried out to validate the present CFD solver. 6DoF motion module is used to predict the trim and sinkage when conducting simulations of ship advancing in calm water. Zha et al.[43] performed numerical predictions of ship resistance with emphasis on viscous wave-making resistance for 6 ship hulls using the present naoe-FOAM-SJTU. Later on, they computed the resistance of high-speed catamaran in calm water[44], where different ship speeds were considered. The numerical results agreed very well with the measurement data of model test. Wave making and vortex field were well simulated and further analysis of the hydrodynamic performance was discussed. Wang et al.[45] further investigated the hydrodynamic performance for a ship with different drift angles. More recently, the CFD solver is applied to simulate breaking wave phenomena of high-speed surface ships[46]. The grid and turbulence model effect on the breaking bow waves were analysed. Figure 14 demonstrates the axial vorticity distributions at three cross sections and the breaking bow wave profile can be easily noticed.

Seakeeping is another key performance of ship hydrodynamics. Based on the developed wave generation and absorption module, various wave conditions can be generated. Incorporating with the 6DOF motion module, ship motions in waves can be estimated by the developed CFD solver. Shen et al.[22] conducted the numerical simulations of ship motion in head waves using RANS approach. Different wave steepness was considered in the simulations and the predicted wave added resistance was validated by the available experimental data. High non-linear phenomena with green water was observed in the computations as shown in Fig. 15. Ye et al.[47] carried out the prediction of wave-added resistance and vertical ship motions for the S-175 ship model. Four wave lengths were simulated to investigate the ship behaviour in different wave conditions. Recently, Liu et al.[48] used naoe-FOAM-SJTU solver to predict more violent conditions for ship motion in waves. The computations were carried out for the benchmark ship model DTC, which is free to heave, pitch and roll, in oblique waves. Dynamic overset grid was adopted to handle with the large ship motions. The mean drift forces and moments on the ship hull can be predicted well even for violent cases with strong wave slamming and large ship motions.

Ship resistance and seakeeping predictions are always done for the bare hull ships. Regarding to free running ship, the complex ship hull-propeller-rudder interaction should be modelled. Based on the developed overset grid module associated with full 6DOF motion with a hierarchy of bodies, applications to free running ship simulations were conducted using naoe-FOAM-SJTU solver. Shen et al.[24] carried out the computations of self-propulsion and zigzag maneuver of KCS ship in calm water, and the predicted self-propulsion parameters as well as maneuvering parameters were compared with the available experimental results. Wang et al.[49] performed the self-propulsion simulation for a twin-screw fully appended ship model and extends to the turning circle maneuver simulations (shown in Fig. 16). The predicted self-propulsion model point matched fairly well with the experimental results and turning parameters were also well predicted with error lower than 10%. Wang et al.[29] further extended the solver to simulate ship maneuvering in waves and the applications for various maneuvers in wave environment using naoe-FOAM-

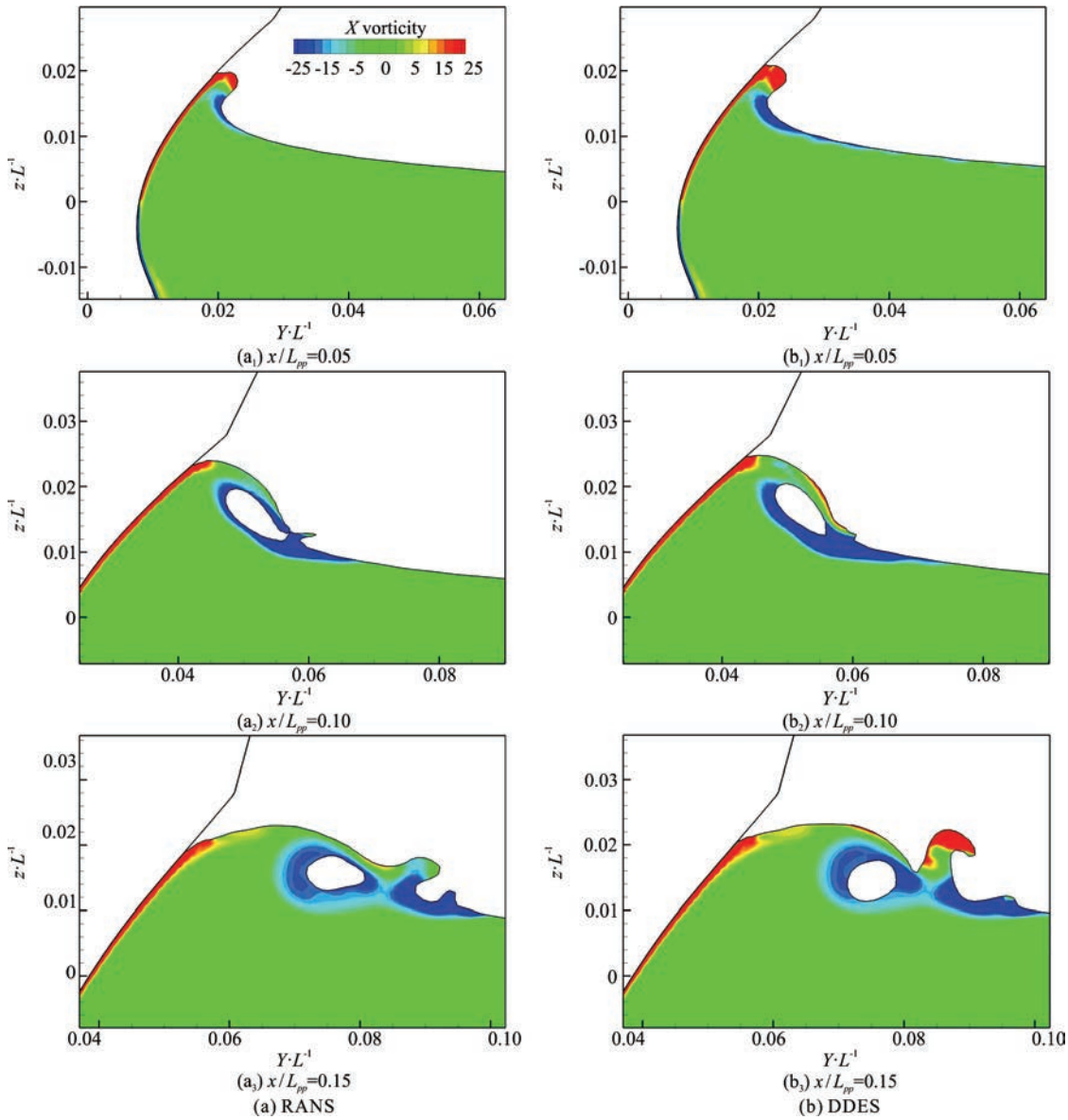

Fig. 14 (Color online) Simulation results of breaking bow waves for a high-speed surface ship[46]

SJTU solver were reviewed in Wang et al.[50]. Therefore, the applications for ship maneuvering in waves are not overviewed herein.

Apart from the investigations of ship resistance, seakeeping, propulsion and maneuvering, naoe-FOAM-SJTU solver has also been applied to estimate the performance of energy save device[51], cavitation, contra-rotating propellers[52], multi-ship interactions, and so on. With the upgrade of the present solver, more and more complex problems in the field of ship hydrodynamics can be numerically studied.

3.2 *Offshore platforms*

The solver has also been applied to various engineering problems for offshore platforms both fixed and floating. For fixed structures, wave run-up is a very important factor for the safe deck design. Cao and Wan[16, 18] carried out benchmark simulations of wave run-up on single cylinder and four cylinders using the current solver. Regular waves with different wave periods and wave heights are studied and wave run-up heights around the cylinders are recorded with virtual wave probes and compared with experimental data. They concluded that naoe-FOAM-SJTU is capable of dealing with wave run-up problems with good accuracy. With the help of 6DOF module, naoe-FOAM-SJTU can predict motions of floating platform in waves. Liu and Wan[53] performed numerical investigations of the motion response of a triple-hulled offshore observation platform with different incident waves. Time histories of motions and loads under different wave conditions are com-

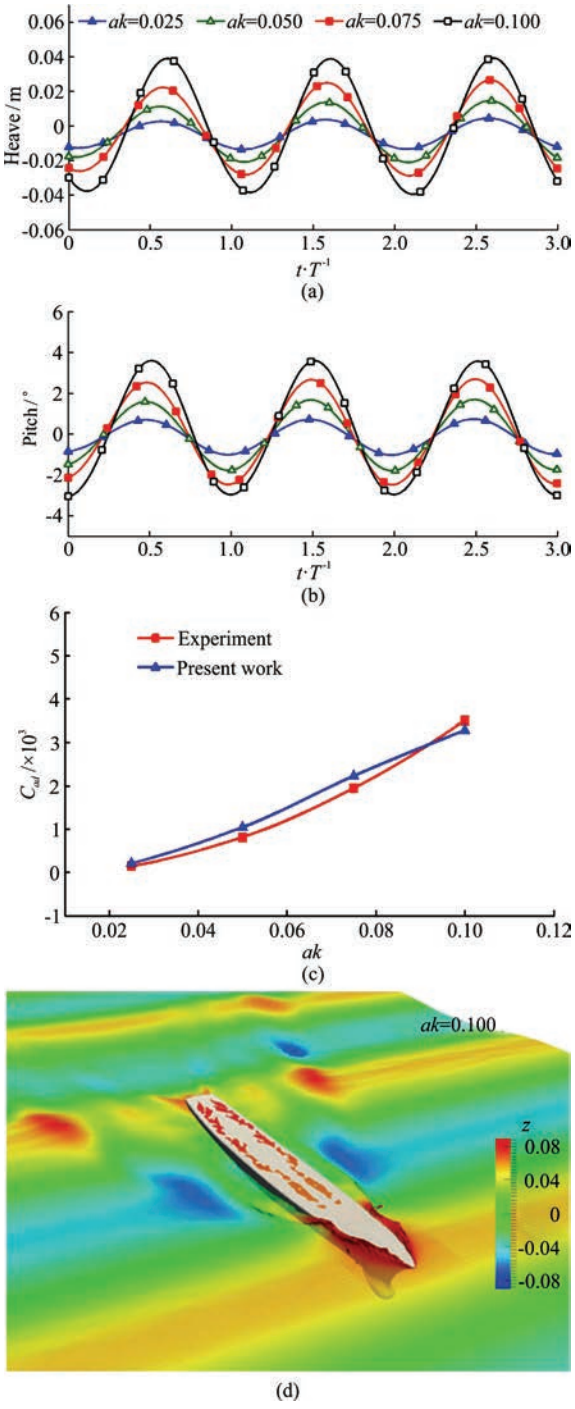

Fig. 15 (Color online) Numerical results of ship motion response ((a), (b)), added wave resistance (c) and instantaneous free surface (d)[22]

pared and analysed. With the help of mooring system module, coupled analysis of floating platform and mooring lines can be performed. Wang and Wan[54] carried out coupled analysis of a floating pie and its mooring system in regular waves. The multicomponent mooring lines are modelled by dynamic analysis lumped mass method (LMM). Motion res-

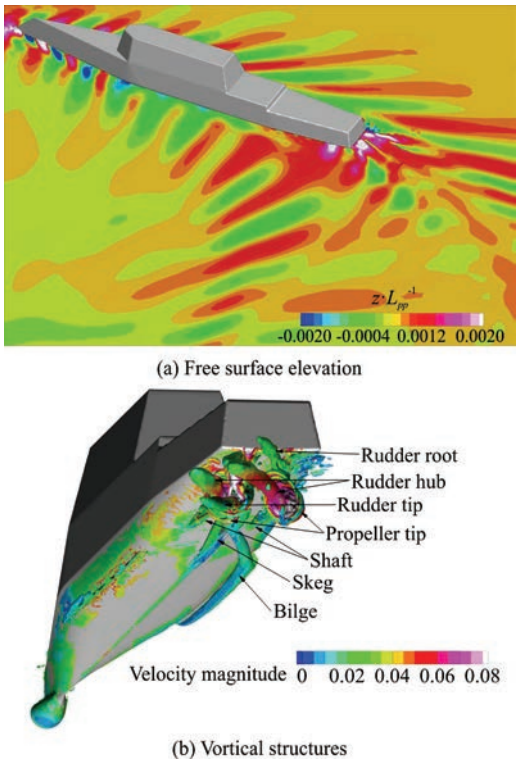

Fig. 16 (Color online) Numerical simulations of turning circle maneuver in calm water[49]

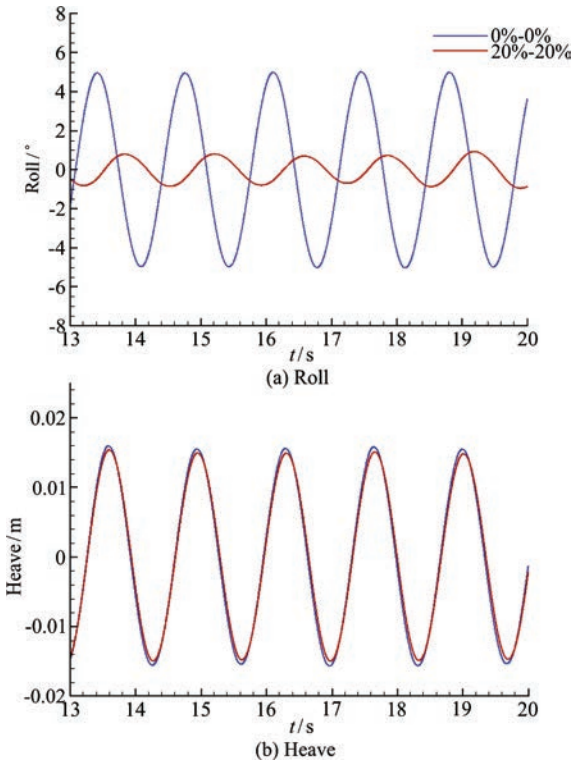

Fig. 17 (Color online) Time histories of heave and roll motions with different filling ratios[58]

ponse were compared with that obtained by the static analysis method. The results showed that dynamic analysis is necessary for coupling analysis between floating platform and mooring system.

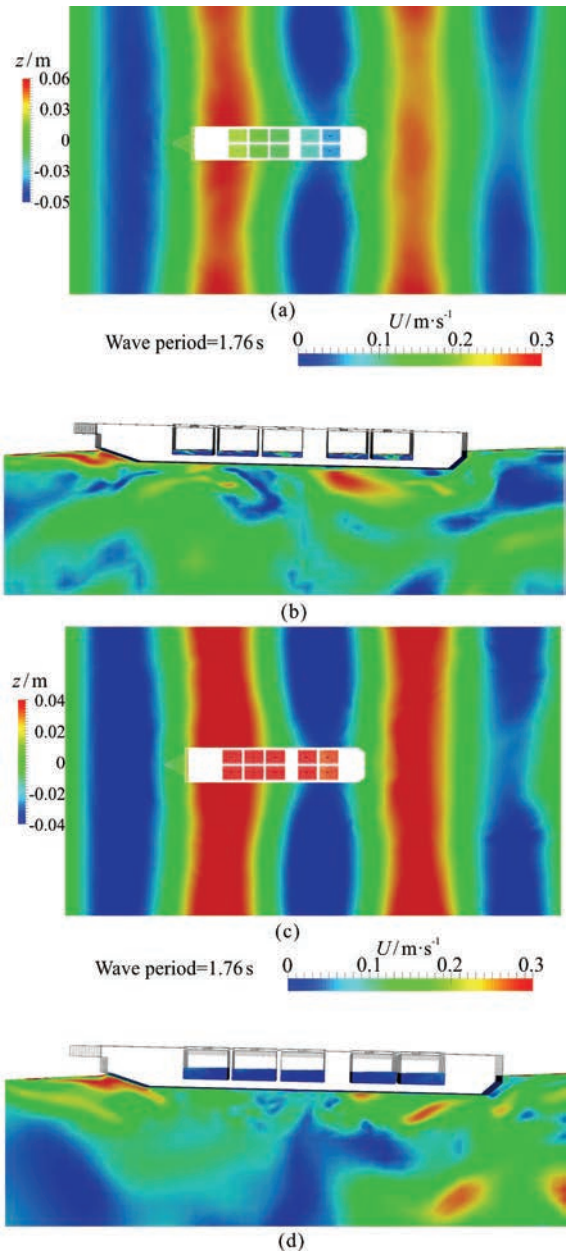

Fig. 18 (Color online) Wave elevation and velocity contour of FLNG hull section under head waves (a), (b) 20% filling ratio (c), (d) 40% filling ratio

Zhuang and Wan[55] studied the motion response of a single-mooring FPSO by utilizing overset grid and mooring system module. The natural periods of both overset and non-overset method for heave decay test were in good agreement with experiment. Motions and mooring forces are further analysed. Wang and Wan[56] also studied the motion characteristics of a single-point moored FPSO under different mooring

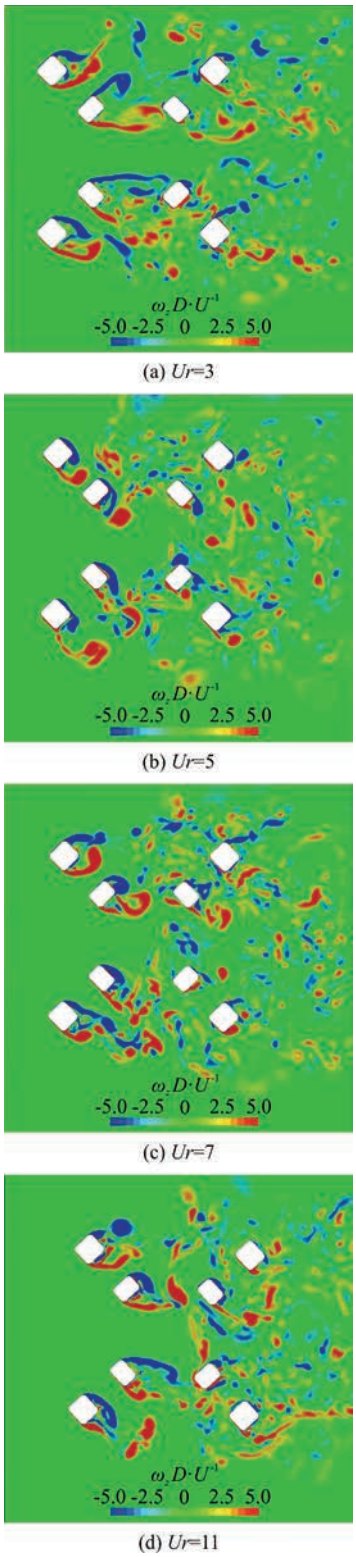

Fig. 19 (Color online) Instantaneous non-dimensional spanwise vorticity contour at different reduced velocities at half draft ($z/L = -0.5$) plane[27]

conditions. Xia and Wan[57] studied the wave evolution and hydrodynamic characteristics of a floating

platform in shallow water with submerged terrain near island. The response amplitude operators (RAOs) of the platform in regular waves were in good agreement with experimental data. Further wave evolution and breaking process over the submerged terrain were depicted and analysed. The naoe-FOAM-SJTU solver can also perform coupled analysis of motion response of an FPSO with sloshing LNG tanks in waves. Zhuang and Wan[58] performed such simulations in which the external wave flow and internal tank sloshing are solved simultaneously. Figure 17 shows the comparison of ship motion between non-filling condition and low-filling condition. The partially filled tanks significantly reduce the roll motion in beam waves. Figure 18 is another case of motion response for an FLNG with 10 tanks in waves. It is shown that the present solver can be applied to predict very complex situations for offshore platforms.

Vortex-induced motions (VIM) is another critical issue for floating offshore platforms with large aspect ratio columns. VIM always occurs with high Reynolds flow and involves massively separated flow. To predict VIM by CFD, the turbulent fluctuation and eddy structures should be resolved properly. The DES can predict massively separated flow at relatively low cost and is adopted by naoe-FOAM-SJTU to predict VIM. Moreover, the complex motion of platform can be handled with the 6DOF module in combination with dynamic overset grid technique. Overall, the solver can be applied to various kinds of floating structures.

Zhao et al.[27] simulated the VIM of a paired-column semi-submersible by using the naoe-FOAM-SJTU solver. The "lock-in" phenomena were captured. Synchronization vortex shedding patterns between upstream columns are observed in the "lock-in" range, as shown in Fig. 19. The transverse motion response and zero crossing period are in good agreement with experiment. Li et al.[59] conducted simulations on VIM of a deep-draft semi-submersible with the current solver. The corner effects of column section shape were discussed. Figure 20 shows the motion trajectories of the platform in horizontal plane. Distinctive motion patterns are observed which indicates the "lock-in" will start earlier with larger column rounded ratios.

Xie et al.[60] used naoe-FOAM-SJTU to simulated the VIM of a single-point moored buoyancy can. The fairlead of the mooring line is in the bottom of the buoyancy can, which results in the barely torque to resist the yaw. To avoid the mesh distortion of large rotation, dynamic overset grid technique is used. The motion trajectory of the buoyancy can shapes a typical "8". The yaw frequency is equal to the transverse motion frequency, which implies the two motions share the same external excitation.

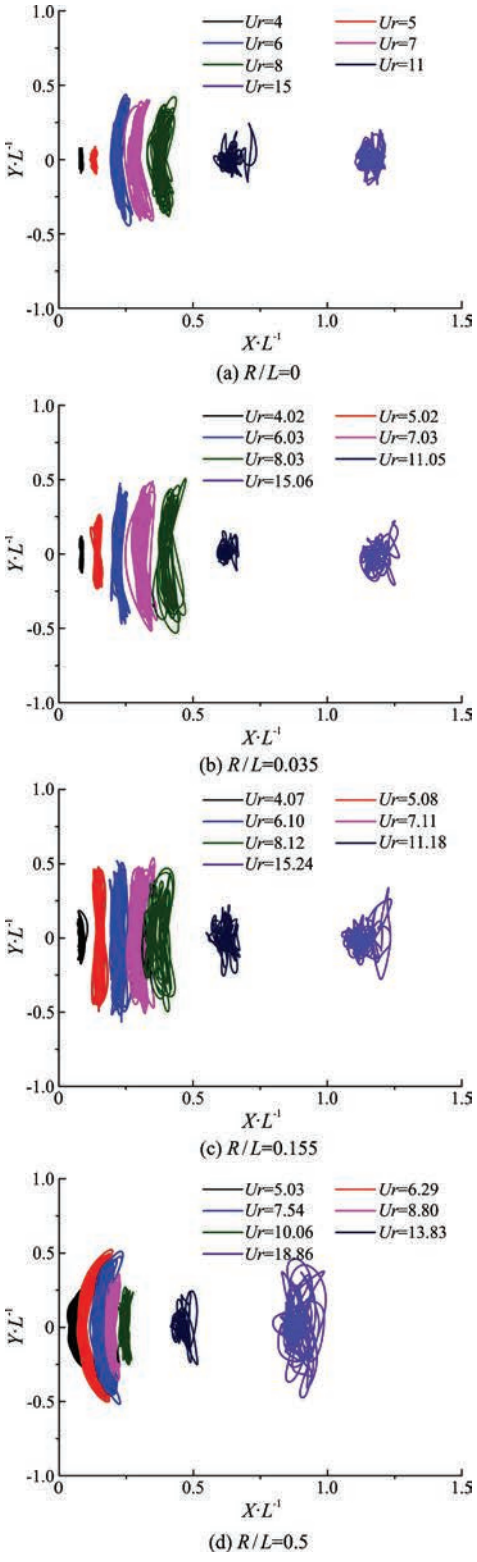

Fig. 20 (Color online) Motion trajectories in the XY plane for the semi-submersibles with different column rounded ratios[59]

3.3 *Marine risers*

The present CFD solver naoe-FOAM-SJTU asso-

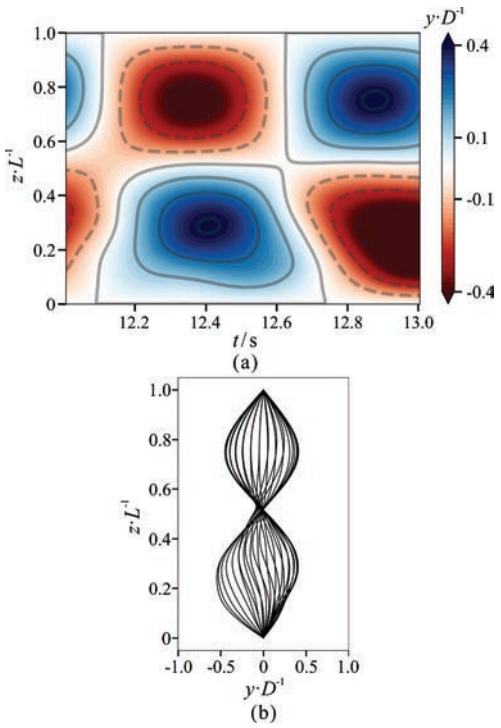

Fig. 21 (Color online) Crossflow non-dimensional spatio-temporal displacement and the deformation envelope line of the riser

ciated with FSI module has been applied to investigate the performance of marine risers under various conditions. Numerical investigations of a flexible riser in stepped flow is carried out using the developed FSI module. The simulation follows the setup of the experiments performed by Chaplin et al.[61]. Figure 21 shows the crossflow non-dimensional spatio-temporal displacement along the flexible riser and the corresponding deformation envelope line. The red to blue colormap represents the positive and negative vibration amplitude. It can be observed that the maximum vibration amplitude occurs at $z/L = 0.25$, 0.75, while the stationary point appears at the mid-span riser. Combining with the deformation envelope line, the vibration of the riser is mainly in the 2nd deformation shape.

Figure 22 shows the crossflow vibration modal weight and the power spectral density (PSD) of each modal weight using the modal decomposition method followed Chaplin et al.[62]. From these figures, it can be known that the 2nd mode is the dominant crossflow vibration mode and the corresponding dominant vibration frequency is around 0.9 Hz for the structural node at the mid-span cylinder. Effects of the 1st and 3rd vibration modes are too small to be considered compared with the 2nd vibration mode, so that the multi-mode vibration phenomenon will not happen

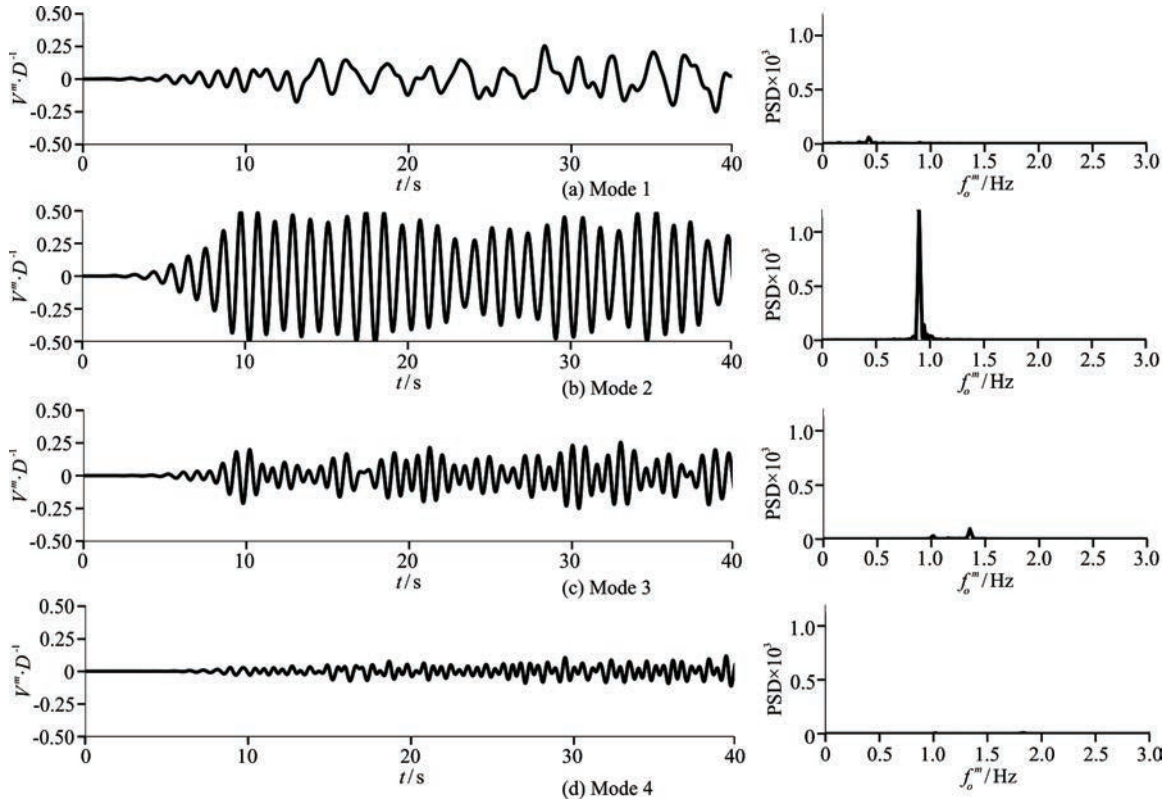

Fig. 22 Crossflow vibration modal weight and PSD at the mid-span riser

under this condition.

In actual oil and gas exploitation, effects of winds, waves and currents will contribute to the periodical oscillation of the offshore platforms, which then leads to the oscillation of the connected riser and the generation of relative oscillatory flow between the riser and the water. Fu et al.[40] employed the developed FSI module with support excitation method to generate the relative oscillatory flow, simulations results were in good agreement with the experimental results and VIV features especially in oscillatory flow had been analysed in detail. Numerical simulations on VIV of a flexible riser exposed to oscillatory flow was conducted adopting the FSI module based on experiments of Fu et al.[63]. Figure 23 showed the non-dimensional crossflow time-dependent displacement at the mid-span cylinder. The specific intermittent VIV developing process of "building up-lock in-dying out"[63] was observed.

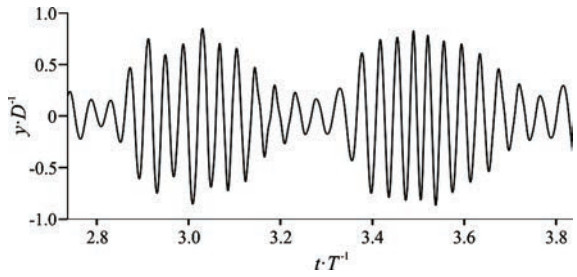

Fig. 23 Non-dimensional crossflow time-dependent displacement at the mid-span riser in an oscillating period[40]

The vibration trajectories at z/L = 0.25, 0.50 and 0.75 of the riser are shown in Fig. 24. The trajectory presents a typical butterfly shape in al structural nodes. Two sides of the butterfly shape are generated when the riser go through the "lock-in" region where the crossflow an inline vibration amplitude get its maximum value at the same time. The central part is generated in the "building-up" and "dying-out" regions where the VIV response in both directions becomes weak with the vibration amplitude decreasing apparently. This butterfly trajectory is also one of the specific phenomena occurred when the riser experiencing oscillatory flow.

In order to promote the oil and gas production, the application of multi-risers becomes more common at present. Compared to the isolated riser condition, the interaction between multi-risers makes the VIV response becoming more complicated. VIV features of two risers have more influencing factors, including the structural parameters of two risers, the flow conditions, the spacing distance and the arrangement. The developed FSI module in naoe-FOAM-SJTU can also manipulate multi-riser simulations. Numerical analysis on VIV of two flexible risers with different arrangements has been carried out. The spacing distance between the centre of two risers is set to be $4D$, while the angle between the centre line of two risers and the incoming flow varies among 0°, 30°, 60° and 90° respectively, as shown in Fig. 25.

Figure 26 shows the wake vortex at different sections of two risers experiencing stepped flow in the tandem arrangement. The development of the wake vortex at the mid-span of two risers is presented in Fig. 27. It can be found that the vortex of the upstream riser will reattach to the surface of the downstream riser, causing the vortex of the downstream riser to be different from that of the isolated riser. Due to the vortex interaction between two risers, VIV features of two risers are quite different from that of the isolated riser. Meanwhile, different arrangements may cause changes in the vibration mode of the riser.

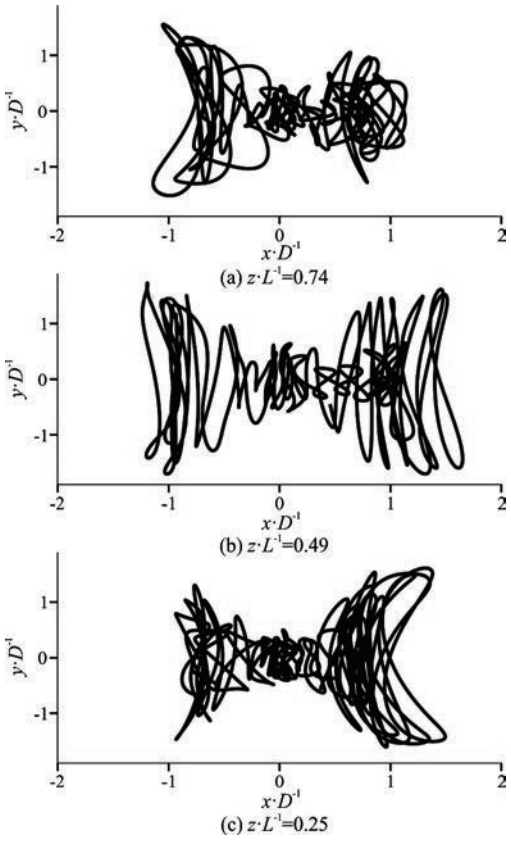

Fig. 24 Vibration trajectories at z/L = 0.25, 0.50 and 0.75 of the riser in an oscillating period[40]

3.4 *Floating offshore wind turbines*

With the rapid development of wind power industry, the floating offshore wind turbines (FOWT) have been paid enough attention. And several floating wind farms have been planned for huge amount offshore wind energy in recent years. There are complex interactions between the aerodynamics of wind turbine and the hydrodynamics of floating plat-

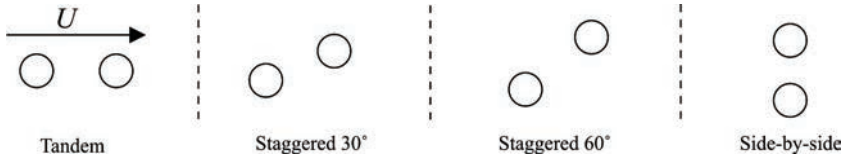

Fig. 25 Layout of two risers in different arrangements

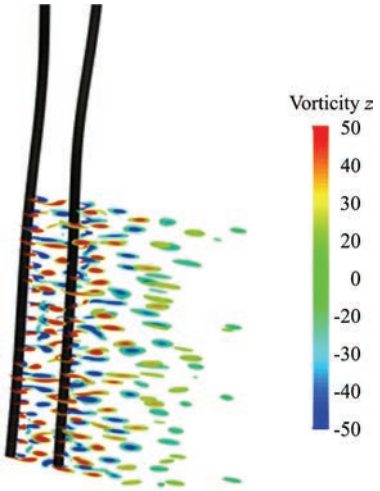

Fig. 26 (Color online) Wake vortex at different sections of two risers

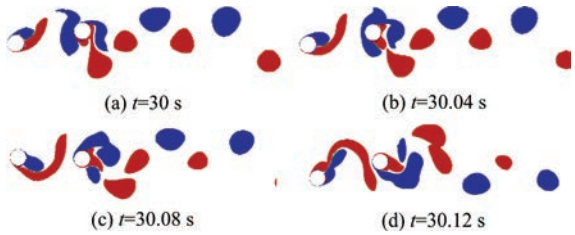

Fig. 27 (Color online) Development of wake vortex at the mid-span of two risers

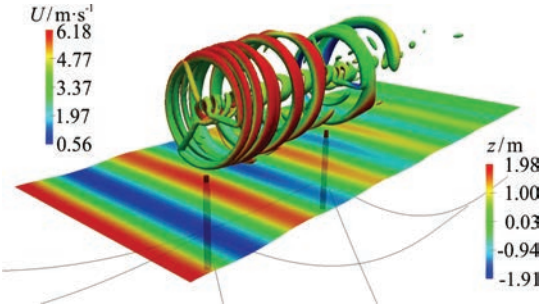

Fig. 28 (Color online) Wake interaction between two spar-type FOWTs using UALM[64]

form, which makes the predictions for the coupled aero-hydrodynamic performance of FOWT are quite challengeable.

By using the coupled CFD analysis tool composed of UALM and naoe-FOAM-SJTU, aero-hydrodynamic simulations for the FOWT under combined wind and wave conditions can be achieved. Many works have been done to investigate the performance of FOWT system in operating ocean environment. To validate the capacity of UALM, the wind turbine aerodynamics restricting the motions of floating platform were firstly carried out. Li et al.[42] studied the wake flow of a semi-submersible FOWT system experiencing prescribed periodic surge and pitch motions. The platform motions were found to have significant effects on the aerodynamic performance of the FOWT. Then coupled aero-hydrodynamic simulations for a FOWT under shear wind and regular wave conditions were carried out[65]. Aerodynamic loads including the rotor power and thrust, motions responses of floating platform and mooring tensions were all obtained from the simulation results. The wake field velocity was obtained, and the vortex structures were also illustra- ted to study the complex wake characteristics of the FOWT. Moreover, the wake interactions between two floating offshore wind turbines were investigated by using this coupled analysis tool[64]. Figure 28 presents the wake interaction between two turbines through the visualizations of vortical structures.

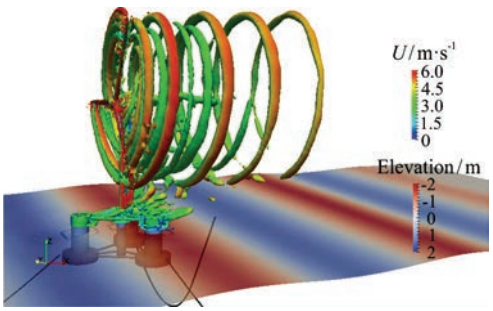

Fig. 29 (Color online) Coupled simulations for OC4 semi-submersible platform system

To obtain more detailed flow field information, the marine hydrodynamic solver naoe-FOAM-SJTU associated with dynamic overset grid technique was employed to investigate the coupled performance of the FOWT system, where the actual rotating blades are considered. Cheng et al.[31, 66-68] performed coupled aero-hydrodynamic simulations for the NREL

5-MW baseline offshore wind turbine mounted on the semi-submersible platform (shown in Fig. 29). The time series of the unsteady torque and thrust were obtained, together with the detailed wake field characteristics, and the pressure coefficient distribution in different cross-section were also available to clarity the detailed flow filed information (shown in Fig. 30). The simulation results showed that the pitch motion had more significant effects on the aerodynamic forces and moments of the rotor than the surge motion does. And the pitch response of floating platform was found to have bad influence on the aerodynamic performance. Besides, the influence of tower effects on the aerodynamic performance of FOWT was also studied.

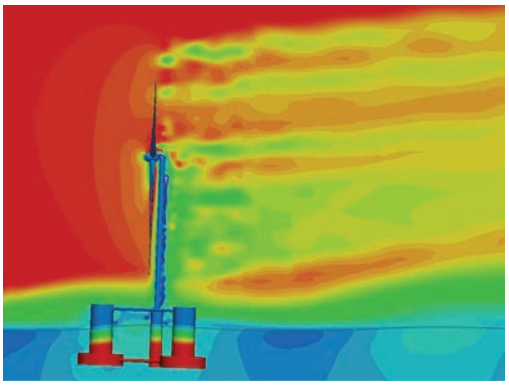

Fig. 30 (Color online) Distribution of the wake flow on a longitudinal section across turbine centre[68]

4. Conclusions

In this paper, the development of CFD solver naoe-FOAM-SJTU based on the open source package OpenFOAM is introduced in detail. The basic features in OpenFOAM for marine hydrodynamics are illustrated at first. The implementation of main modules in naoe-FOAM-SJTU including wave generation and absorption, 6DOF motion with a hierarchy of bodies, mooring system, dynamic overset grid, fluid-structure interaction and unsteady actuator line model are presented. Extensive applications in marine hydrodynamic problems are discussed focusing on ship hydrodynamics, offshore platforms, marine risers and floating offshore wind turbines. It is concluded that with the development of specified modules in OpenFOAM, the present naoe-FOAM-SJTU solver can deal with many of the marine hydrodynamic problems.

Future work will focus on two parts, one is the improvement of existing modules and another one is the extension of the present solver by involving more modules for marine hydrodynamics. Emphasis is put on the efficiency and accuracy of the present modules to improve reliability of the CFD solver. More modules, including coupling strategy between potential flow and viscous flow, ship optimization design, are considered to extend the ability of naoe-FOAM-SJTU for marine hydrodynamics.

Acknowledgements

This work was supported by the Chang Jiang Scholars Program (Grant No. T2014099), the Shanghai Excellent Academic Leaders Program (Grant No. 17XD1402300), the Program for Professor of Special Appointment (Eastern Scholar) at Shanghai Institutions of Higher Learning (Grant No. 2013022) the Innovative Special Project of Numerical Tank of Ministry of Industry and Information Technology of China (Grant No. 2016-23/09) and Lloyd's Register Foundation for doctoral student, to which the authors are most grateful.

References

[1] Jasak H., Jemcov A., Tukovic Z. et al. OpenFOAM: A C++ library for complex physics simulations [C]. *Proceedings of International workshop on coupled methods in numerical dynamics*, Dubrovnik, Croatia, 2007, 1-20.

[2] Jasak H. OpenFOAM: Open source CFD in research and industry [J]. *International Journal of Naval Architecture and Ocean Engineering*, 2009, 1(2): 89-94.

[3] Kunkelmann C., Stephan P. CFD simulation of boiling flows using the volume-of-fluid method within OpenFOAM [J]. *Numerical Heat Transfer, Part A: Applications*, 2009, 56(8): 631-646.

[4] Magnini M., Pulvirenti B., Thome J. R. Numerical investigation of hydrodynamics and heat transfer of elongated bubbles during flow boiling in a microchannel [J]. *International Journal of Heat and Mass Transfer*, 2013, 59: 451-471.

[5] Higuera P., Lara J. L., Losada I. J. Simulating coastal engineering processes with OpenFOAM® [J]. *Coastal Engineering*, 2013, 71: 119-134.

[6] Horgue P., Soulaine C., Franc J. et al. An open-source toolbox for multiphase flow in porous media [J]. *Computer Physics Communications*, 2015, 187: 217-226.

[7] Larsen B. E., Fuhrman D. R. On the over-production of turbulence beneath surface waves in Reynolds-averaged Navier-Stokes models[J]. *Journal of Fluid Mechanics*, 2018, 853: 419-460.

[8] So K. K., Hu X. Y., Adams N. A. Anti-diffusion interface sharpening technique for two-phase compressible flow simulations [J]. *Journal of Computational Physics*, 2012, 231(11): 4304-4323.

[9] Jacobsen N. G., Fuhrman D. R., Fredsøe J. A wave generation toolbox for the open-source CFD library: OpenFoam® [J]. *International Journal for Numerical Methods in Fluids*, 2012, 70(9): 1073-1088.

[10] Duanmu Y., Zou L., Wan D. C. Numerical simulations of vortex-induced vibrations of a flexible riser with different aspect ratiosin uniform and shear currents [J]. *Journal of Hydrodynamics*, 2017, 29(6): 1010-1022.

[11] Jasak H. Dynamic mesh handling in OpenFOAM [C]. *47th*

AIAA Aerospace Sciences Meeting Including the New Horizons Forum and Aerospace Exposition. Orlando, Florida, USA, 2009.
[12] Berberović E., van Hinsberg N., Jakirlić S. et al. Drop impact onto a liquid layer of finite thickness: Dynamics of the cavity evolution[J]. *Physical Review E*, 2009, 79(3): 36306.
[13] Zhao W., Wan D. C. Detached-eddy simulation of flow past tandem cylinders [J]. *Applied Mathematics and Mechanics*, 2016, 37(12): 1272–1281.
[14] Issa R. I. Solution of the implicitly discretised fluid flow equations by operator-splitting [J]. *Journal of Computational Physics*, 1986, 62(1): 40-65.
[15] Higuera P., Lara J. L., Losada I. J. Realistic wave generation and active wave absorption for Navier-Stokes models: Application to OpenFOAM® [J]. *Coastal Engineering*, 2013, 71: 102-118.
[16] Cao H., Wan D. C. Benchmark computations of wave run-up on single cylinder and four cylinders by naoe-FOAM-SJTU solver [J]. *Applied Ocean Research*, 2017, 65: 327-337.
[17] Cao H., Wan D. C. Development of multidirectional nonlinear numerical wave tank by naoe-FOAM-SJTU solver [J]. *International Journal of Ocean System Engineering*, 2014, 4(1): 52-59.
[18] Cao H., Wan D. C. RANS-VOF solver for solitary wave run-up on a circular cylinder [J]. *China Ocean Engineering*, 2015, 29(2): 183-196.
[19] Cox D. T., Ortega J. A. Laboratory observations of green water overtopping a fixed deck [J]. *Ocean Engineering*, 2002, 29(14): 1827-1840.
[20] Shen Z., Wan D. C. An irregular wave generating approach based on naoe-FOAM-SJTU solver [J]. *China Ocean Engineering*, 2016, 30: 177-192.
[21] Cao H., Zha J., Wan D. C. Numerical simulation of wave run-up around a vertical cylinder [C]. *The Twenty-first International Offshore and Polar Engineering Conference*. Maui, Hawaii, USA, 2011, 726-733.
[22] Shen Z., Wan D. C. RANS computations of added resistance and motions of a ship in head waves [J]. *International Journal of Offshore and Polar Engineering*, 2013, 23(4): 264-271.
[23] Liu Y., Wan D. C. Numerical simulation of motion response of an offshore observation platform in waves [J]. *Journal of Marine Science and Application*, 2013, 12(1): 89-97.
[24] Shen Z., Wan D. C., Carrica P. M. Dynamic overset grids in OpenFOAM with application to KCS self-propulsion and maneuvering [J]. *Ocean Engineering*, 2015, 108: 287-306.
[25] Liu Y., Xiao Q., Incecik A. et al. Establishing a fully coupled CFD analysis tool for floating offshore wind turbines [J]. *Renewable Energy*, 2017, 112: 280-301.
[26] Zhuang Y., Wan D. C. Numerical study on ship motion fully coupled with LNG tank sloshing in CFD method [J]. *International Journal of Computational Methods*, 2017, 1840022.
[27] Zhao W., Zou L., Wan D. C. et al. Numerical investigation of vortex-induced motions of a paired-column semi-submersible in currents [J]. *Ocean Engineering*, 2018, 164: 272-283.
[28] Liu Y., Xiao Q., Atilla I. et al. Investigation of the effects of platform motion on the aerodynamics of a floating offshore wind turbine [J]. *Journal of Hydrodynamics*, 2016, 28(1): 95-101.
[29] Wang J., Zou L., Wan D. C. CFD simulations of free running ship under course keeping control [J]. *Ocean Engineering*, 2017, 141: 450-464.
[30] Wang J., Zou L., Wan D. C. Numerical simulations of zigzag maneuver of free running ship in waves by RANS-Overset grid method [J]. *Ocean Engineering*, 2018, 162: 55-79.
[31] Cheng P., Wan D. C. Fully-coupled aero-hydrodynamic simulation of floating offshore wind turbines by different simulation methods [C]. *ASME 2018 37th International Conference on Ocean, Offshore and Arctic Engineering*, 2018, V11AT12A045.
[32] Noack R. W., Boger D. A., Kunz R. F. et al. Suggar++: An improved general overset grid assembly capability [C]. *Proceedings of the 19th AIAA Computational Fluid Dynamics Conference*, San Antonio, TX, USA, 2009, 22-25.
[33] Carrica P. M., Huang J., Noack R. et al. Large-scale DES computations of the forward speed diffraction and pitch and heave problems for a surface combatant [J]. *Computers and Fluids*, 2010, 39(7): 1095-1111.
[34] Willden R. H. J., Graham J. M. R. Numerical prediction of VIV on long flexible circular cylinders [J]. *Journal of Fluids and Structures*, 2001, 15(3-4): 659-669.
[35] Willden R. H., Graham J. M. R. Multi-modal vortex-induced vibrations of a vertical riser pipe subject to a uniform current profile [J]. *European Journal of Mechanics-B/Fluids*, 2004, 23(1): 209-218.
[36] Yamamoto C. T., Meneghini J. R., Saltara F. et al. Numerical simulations of vortex-induced vibration on flexible cylinders [J]. *Journal of Fluids and Structures*, 2004, 19(4): 467-489.
[37] Meneghini J. R., Saltara F., Fregonesi R. D. A. et al. Numerical simulations of VIV on long flexible cylinders immersed in complex flow fields [J]. *European Journal of Mechanics - B/Fluids*, 2004, 23(1): 51-63.
[38] Duanmu Y., Zou L., Wan D. C. Numerical analysis of multi-modal vibrations of a vertical riser in step currents [J]. *Ocean Engineering*, 2018, 152: 428-442.
[39] Fu B., Zou L., Wan D. C. Numerical study on the effect of current profiles on vortex-induced vibrations in a top-tension riser [J]. *Journal of Marine Science and Application*, 2017, 16(4): 473-479.
[40] Fu B., Zou L., Wan D. C. Numerical study of vortex-induced vibrations of a flexible cylinder in an oscillatory flow [J]. *Journal of Fluids and Structures*, 2018, 77: 170-181.
[41] Sørensen J. N., Shen W. Z. Numerical modeling of wind turbine wakes [J]. *Journal of Fluids Engineering*, 2002, 124(2): 393-399.
[42] Li P., Cheng P., Wan D. C. Numerical simulations of wake flows of floating offshore wind turbines by unsteady actuator line model [C]. *The 9th International Workshop on Ship and Marine Hydrodynamics*, Glasgow, UK, 2015.
[43] Zha R., Ye H., Shen Z. et al. Numerical study of viscous wave-making resistance of ship navigation in still water [J]. *Journal of Marine Science and Application*, 2014, 13(2): 158-166.
[44] Zha R., Ye H., Shen Z. et al. Numerical computations of resistance of high speed catamaran in calm water [J]. *Journal of Hydrodynamics*, 2015, 26(6): 930-938.
[45] Wang J., Liu X., Wan D. C. Numerical simulation of an oblique towed ship by naoe-FOAM-SJTU solver [C]. *Proceedings of 25th International Offshore and Polar Engineering Conference*, Big Island, Hawaii, USA, 2015.
[46] Wang J., Ren Z., Wan D. C. RANS and DDES computations of high speed KRISO container ship [C]. *Procee-*

dings of the 32nd Symposium on Naval Hydrodynamics, Hamburg, Germany, 2018.
[47] Ye H., Shen Z., Wan D. C. Numerical prediction of added resistance and vertical ship motions in regular head waves [J]. *Journal of Marine Science and Application*, 2012, 11(4): 410-416.
[48] Liu C., Wang J., Wan D. C. CFD Computation of wave forces and motions of DTC ship in oblique waves [J]. *International Journal of Offshore and Polar Engineering*, 2018, 28(2): 154-163.
[49] Wang J., Zhao W., Wan D. C. Free maneuvering simulation of ONR tumblehome using overset grid method in naoe-FOAM-SJTU solver [C]. *Proceedings of 31th Symposium on Naval Hydrodynamics*, Monterey, USA, 2016.
[50] Wang J., Wan D. C. CFD Investigations of ship maneuvering in waves using naoe-FOAM-SJTU solver [J]. *Journal of Marine Science and Application*, 2018, 17(3): 443-458.
[51] Sun T., Wan D. C. Study of energy saving effect for preduct [J]. *Chinese Journal of Hydrodynamics*. 2016, 31(6): 651-658(in Chinese).
[52] He D., Wan D. C. Investigations of hydrodynamic performance of contra-rotating propellers with different design parameters [J]. *The Ocean Engineering*, 2018, 36(2): 19-29(in Chinese).
[53] Liu Y., Wan D. C. Numerical simulation of motion response of an offshore observation platform in waves [J]. *Journal of Marine Science and Application*, 2013, 12(1): 89-97.
[54] Wang J., Wan D. C. Dynamic coupling analysis of the mooring system and floating pier in the South China Sea [J]. *Chinese Journal of Hydrodynamics*, 2015, 30(2): 180-186(in Chinese).
[55] Zhuang Y., Wan D. C. Numerical study of single point mooring system FPSO based on overset grids [J]. *Journal of Jiangsu University of Science and Technology (Natural Science Edition)*, 2017, 31(5): 574-578(in Chinese).
[56] Wang D., Wan D. C. CFD Simulations of single point mooring FPSO in waves [J]. *Shipbuilding of China*, 2017, 58(S1): 36-43(in Chinese).
[57] Xia K., Wan D. C. Numerical investigation of motion response of floating platform near submerged terrain [J]. *The Ocean Engineering*, 2018, 36(3): 10-17(in Chinese).
[58] Zhuang Y., Wan D. C. Numerical study on coupling effects of FPSO ship motion and LNG tank sloshing in low-filling condition [J]. *Applied Mathematics and Mechanics*, 2016, 37(12): 1378-1393.
[59] Li S., Zhao W., Wan D. C. Numerical study of column rounded corner effects on vortex-induced motions of semi-submersibles [C]. *The Thirteenth (2018) Pacific-Asia Offshore Mechanics Symposium*, Jeju, Korea, 2018, 120-128.
[60] Xie K., Zhao W., Wan D. C. naoe-FOAM-SJTU solver for numerical study of vortex-induced motions of a buoyancy can in currents [J]. *Journal of Shipping and Ocean Engineering*, 2017, 6: 223-232.
[61] Chaplin J. R., Bearman P. W., Huarte F. H. et al. Laboratory measurements of vortex-induced vibrations of a vertical tension riser in a stepped current [J]. *Journal of Fluids and Structures*, 2005, 21(1): 3-24.
[62] Chaplin J. R., Bearman P. W., Cheng Y. et al. Blind predictions of laboratory measurements of vortex-induced vibrations of a tension riser [J]. *Journal of Fluids and Structures*, 2005, 21(1): 25-40.
[63] Fu S., Wang J., Baarholm R. et al. VIV of flexible cylinder in oscillatory flow [C]. *ASME 2013 32nd International Conference on Ocean, Offshore and Arctic Engineering*, Nantes, France, 2013, V007T08A021.
[64] Huang Y., Cheng P., Wan D. C. Numerical analysis on two floating offshore wind turbines with different layouts [C]. *The 9th International Conference on Computational Methods*, Rome, Italy, 2018.
[65] Li P., Wan D. C., Liu J. Numerical simulations of wake flows of wind turbine based on actuator line model [J]. *Chinese Journal of Hydrodynamics*, 2016, 31(2): 127-134(in Chinese).
[66] Cheng P., Wan D. C., Hu C. Unsteady aerodynamic simulations of floating offshore wind turbines with overset grid technology [C]. *The 26th International Ocean and Polar Engineering Conference*, Rhodes, Greece, 2016, 391-398.
[67] Cheng P., Wan D. C. Analysis of wind turbine blade-tower interaction using overset grid method [J]. *Chinese Journal of Hydrodynamics*, 2017, 32(1): 32-39(in Chinese).
[68] Cheng P., Wan D. C., Hu C. Numerical simulations of flows around floating offshore wind turbine [C]. *The 28th International Ocean and Polar Engineering Conference*, Sapporo, Japan, 2018, 414-421.

OFW13 Website: http://dcwan.sjtu.edu.cn/OpenFOAM2018/